



Low-frequency anomalies of seismic-wave reflections from poroelastic layers

Beatriz Quintal*, Geological Institute, ETH Zurich, Switzerland

Stefan M. Schmalholz, Geological Institute, ETH Zurich, Switzerland

Yuri Y. Podladchikov, Physics of Geological Processes (PGP), University of Oslo, Norway

José M. Carcione, Istituto Nazionale di Oceanografia e di Geofisica Sperimentale (OGS), Italy

Copyright 2007, SBGf - Sociedade Brasileira de Geofísica

This paper was prepared for presentation at the 10th International Congress of The Brazilian Geophysical Society held in Rio de Janeiro, Brazil, 19-22 November 2007.

Contents of this paper were reviewed by the Technical Committee of the 10th International Congress of the Brazilian Geophysical Society and do not necessarily represent any position of the SBGf, its officers or members. Electronic reproduction, or storage of any part of this paper for commercial purposes without the written consent of the Brazilian Geophysical Society is prohibited.

Abstract

Low-frequency (1-10 Hz) reflection anomalies can be related to hydrocarbon-saturated rocks with anomalous high values of attenuation. We study low-frequency reflections from a poroelastic layered reservoir, which is embedded in an elastic background medium, using Biot's theory and 1D finite-difference modeling of wave propagation. The reservoir has a constant thickness and consists of a variable number of two different alternating fluid-saturated layers. For few layers the reflections from the reservoir are identical when we compare results for poroelastic layers with results for equivalent elastic layers. For many layers, i.e. thinly-layered reservoir, the results are considerably different. In the elastic case, the reflections disappear, because we have chosen the impedance of the background medium similar to the Backus-averaged (no-flow limit) impedance of the reservoir. In the poroelastic case, we observe considerable reflections, caused by velocity dispersion as a result of wave-induced viscous fluid flow and attenuation between layers.

Introduction

Recently, *Korneev et al.* [2004] showed that reflections from fluid-saturated layers have increased amplitude and delayed travel time when compared with reflections from gas-saturated layers. They consider laboratory and field measurements in the kHz and 1-20 Hz range, and explain the observed frequency-dependent reflections in the kHz range with very low values of the quality factor (< 5) within the layers. They model low values of the quality factor by adding a diffusive term in the 1D elastodynamic wave equation, stating that the attenuation mechanism is still unclear. Their simple model predicts fairly well the low-frequency dependence of field data, considering the difference between reflections from a reservoir, measured during summer (gas filled) and winter (water filled).

Goloshubin et al. [2006] used some examples of field data processing to show that the use of seismic imaging at low frequencies has a strong potential for prognoses of fluid content and for mapping of productive highly permeable zones of reservoirs. They suggest the possibility of calibrating seismic frequency-dependent reflectivity measurements to reservoir properties in new processing techniques.

High values of attenuation (i.e. low values of quality factor) in hydrocarbon-saturated layers have often been observed, and related reflections in the low-frequency range have recently attracted an increased interest in the scientific and industrial communities [e.g., *Chapman et al.*, 2006; *Goloshubin et al.*, 2006; *Graf et al.*, 2007]. Here, we investigate reflections from a reservoir with low values of the quality factor, using a physically-based model for low-frequency wave attenuation, which is often referred to as one-dimensional (1D) interlayer-flow model [*White et al.*, 1975; *Norris*, 1993; *Gurevich and Lopatnikov*, 1995; *Müller and Gurevich*, 2004; *Carcione and Picotti*, 2006; *Carcione*, 2007]. This model is a particular 1D version of the so-called patchy-saturation models [e.g., *White*, 1975; *Carcione et al.*, 2003; *Pride et al.*, 2004; *Toms et al.*, 2006]. In these models, attenuation and velocity dispersion are caused by wave-induced viscous (dissipative) fluid flow, generated by fluid pressure differences in heterogeneous, saturated poroelastic materials. The wave propagation in such saturated poroelastic materials can be described mathematically with Biot's equations [*Biot*, 1962; *Dutta and Odé*, 1979a, 1979b; *Bourbié*, 1987; *Carcione*, 2007].

It is known that only at frequencies higher than 100 KHz, the standard Biot's visco-inertial attenuation mechanism (Biot, 1962; Bourbié et al., 1987) may contribute to the overall attenuation in a layered poroelastic rock. For lower frequencies the dynamic effects can be ignored and Gassmann theory applies. A fundamental assumption of Gassmann theory is that, if frequency is sufficiently low, then fluid everywhere in the rock is in pressure equilibrium. In a homogeneous fully-saturated rock this is simply the case. However, in partially saturated rocks, the wave passing through the heterogeneities induces spatial gradients in fluid pressure, and this causes viscous losses due to fluid flow. Wave induced-flow of the pore fluid between heterogeneities of mesoscale (small compared to the wavelength and large compared to the typical pore size) are the major cause of elastic wave attenuation and dispersion, in the low frequency range of seismic waves.

Several laboratory experiments with porous rocks provide evidence of the existence of mesoscopic saturation heterogeneities, e.g. *Cadore et al.* [1998].

The interlayer-flow model, using realistic reservoir properties as model parameters, is able to predict low values of the quality factor and significant velocity dispersion within the low 1-10 Hz frequency range [Carcione and Picotti, 2006]. However, the unbounded analytical model, consisting of two alternating layers, cannot be used to evaluate the reflection coefficient of a finite layered reservoir and we, therefore, apply finite-difference simulations of wave propagation.

In our setup, the reservoir has constant thickness and is composed of a variable number of pairs of layers (Figure 1). Each pair consists of one layer with slightly higher and one layer with slightly lower effective impedance than the background medium. One purpose of using this particular model is to evaluate the range of applicability of the analytical solution based on an infinite number of pairs of layers [White et al., 1975].

A particular focus of this study is to model two physical transitions that are caused by the increase of the number of layers, which are first, the transition from a heterogeneous reservoir (i.e. coarsely-layered) to an effective homogeneous reservoir (finely-layered where Backus averaging is applicable), and second, the transition from the no-flow, high-frequency limit, to the quasi-static, low-frequency limit.

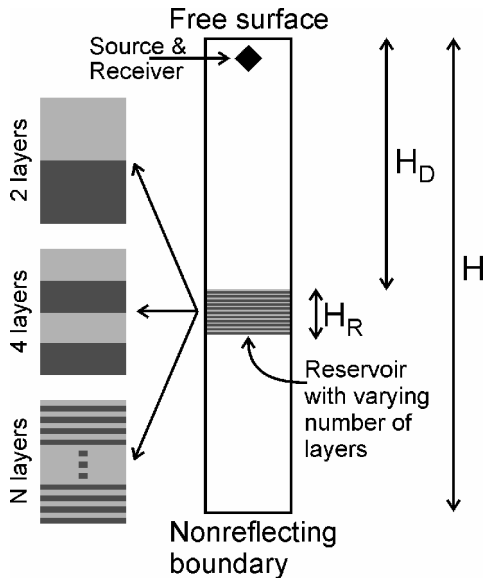


Figure 1. Model setup. The white part represents the elastic background medium, the grey layer is the water-saturated and the black layer is the gas-saturated. H_D is 300 m, H_R is 100 m and H is 400 m.

Equation of motion and numerical method

We use the elastodynamic equations and Biot's equations [Biot, 1962] to model wave propagation in elastic and poroelastic media, respectively, expressed as a first-order velocity-stress formulation [Levander, 1988]. Only the poroelastic equations are shown here. The solid particle velocity U_z , the fluid relative to the solid velocity W_z , the

solid stress τ_{zz} and pore-fluid pressure p_f are the four unknowns in the four equations describing poroelastic wave propagation:

$$(m\rho - \rho_f^2) \frac{\partial U_z}{\partial t} = m \frac{\partial \tau_{zz}}{\partial z} + \rho_f \frac{\partial p_f}{\partial z} + \rho_f \frac{\eta}{k} W_z + S,$$

$$(\rho_f^2 - \rho m) \frac{\partial W_z}{\partial t} = \rho_f \frac{\partial \tau_{zz}}{\partial z} + \rho \frac{\partial p_f}{\partial z} + \rho \frac{\eta}{k} W_z,$$

$$\frac{\partial \tau_{zz}}{\partial t} = (2\mu + \lambda_c) \frac{\partial U_z}{\partial z} + \alpha M \frac{\partial W_z}{\partial z},$$

$$\frac{\partial p_f}{\partial t} = -\alpha M \frac{\partial U_z}{\partial z} - M \frac{\partial W_z}{\partial z},$$

where t is the time, z is the vertical coordinate, S is a source term, ρ is the composite density of the saturated medium, ρ_f is the fluid density, m is the effective fluid density, η is the fluid viscosity, k is the permeability, and μ and λ_c are the Lamé parameters, the former being the shear modulus of the dry porous frame. The parameters α and M are defined as

$$\alpha = 1 - K_b / K_s,$$

$$M = [\phi / K_f + (\alpha - \phi) / K_s]^{-1},$$

where K_b is the bulk modulus of the dry porous frame, K_s is the bulk modulus of the solid material and K_f is the bulk modulus of the pore fluid. The composite density of the saturated medium is calculated through

$$\rho = (1 - \phi) \rho_s + \phi \rho_f,$$

where ρ_s is the density of the solid material and ϕ is the porosity. The effective fluid density is given by

$$m = T \rho_f / \phi,$$

where $T = 1 - r(1 - 1/\phi)$ is the tortuosity, a parameter related to the pore structure, and we use $r = 0.5$, which corresponds to spherical grains [Berryman, 1980]. The Lamé parameter λ_c can be determined through the formula

$$\lambda_c = K_c - 2\mu/3,$$

where K_c is the bulk modulus of the saturated medium, which is related to the parameters K_b , α and M [Bourbié et al., 1987; Carcione, 2007] through

$$K_c = K_b + \alpha^2 M.$$

The four poroelastic equations are solved with an explicit finite-difference scheme using staggering in both space and time. For the poroelastic equations, we use a partition scheme [Carcione and Quiroga-Goode, 1995]. The difference operators are second-order accurate in time and space. We successfully tested the numerical scheme versus analytical solutions of phase velocity and quality factor [e.g., White et al., 1975; Carcione and Picotti, 2006] (Figure 4). The quality factor was calculated using the spectral-ratio and frequency-shift methods [Toksöz et al.,

1979; *Quan and Harris, 1997; Picotti and Carcione, 2006*].

Numerical Experiments

The numerical model setup is shown in Figure 1. Source and receiver are located at the same position, at the top of the model. The source is a Gaussian pulse in time with maximum amplitude occurring at 0.1 s and characteristic e-fold decay frequency of 12 Hz. The receiver records the solid particle velocities during the total time of 2s. A free surface is implemented at the top of the model and a non-reflecting boundary at the bottom. The petrophysical properties are given in Table 1. For the poroelastic simulations the background medium is effectively elastic (porosity is set to 0.01 and fluid viscosity to 1 Pa s). The reservoir is always 100 m thick and we vary only the number of layers so that the thicknesses decrease with increasing number of layers.

Table 1. Material properties.

	Background medium	Water-saturated layer	Gas-saturated layer
K_b	6.6 GPa	6.6 GPa	6.6 GPa
K_s	8.588 GPa	28.9 GPa	28.9 GPa
K_f	2.3 GPa	2.3 GPa	0.022 GPa
ϕ	0.001	0.2	0.2
ρ_s	2360 kg/m ³	2700 kg/m ³	2700 kg/m ³
ρ_f	1000 kg/m ³	1000 kg/m ³	140 kg/m ³
μ	5.6 GPa	5.6 GPa	5.6 GPa
k	50 mD	50 mD	50 mD
η	1 Pa s	0.003 Pa s	10 ⁻⁵ Pa s

For the elastic simulations, we calculate the equivalent P-wave velocities and composite densities using low-frequency Gassmann's equations (< 10 Hz) [*Gassmann, 1951; Bourbié et al., 1987; Carcione, 2007*].

We compute the Fourier spectra of the recorded particle velocity using the fast Fourier transform of MATLAB (© 1994-2006 The MathWorks, Inc.), and analyze the spectral anomalies which are caused by waves propagating between the reservoir and the free surface due to multiple reflections. Figure 2 shows the normalized spectra corresponding to 2, 32 and 500 layers. The normalization is done by dividing each spectrum by the spectrum of the particle velocity recorded in a simulation with no reservoir (homogeneous background medium only). The spectra for the elastic and poroelastic cases are identical for 2 layers (Figure 2a), but increasing the number of layers, e.g. 32 layers (Figure 2b), causes a decrease of the amplitudes of spectral anomalies. Increasing the number of layers to 500 (Figure 2c) yields a spectrum for the poroelastic case remarkably different, compared to the one for the elastic case.

To compare the spectral anomalies for the elastic and poroelastic cases, we define a peak strength (vertical

lines plotted in Figure 2), which corresponds to the average vertical height of the spectral anomaly. Figure 3 shows peak strengths for the spectral anomalies at about 8 Hz, resulting from numerical simulations performed for 2, 8, 16, 32, 64, 128, 256, 500, 1000 and 2000 elastic and poroelastic layers. The peak strength for the elastic case decreases continuously with increasing number of layers, but the peak strength corresponding to the poroelastic case first decreases and then increases with increasing number of layers, until it saturates at about 1000 layers.

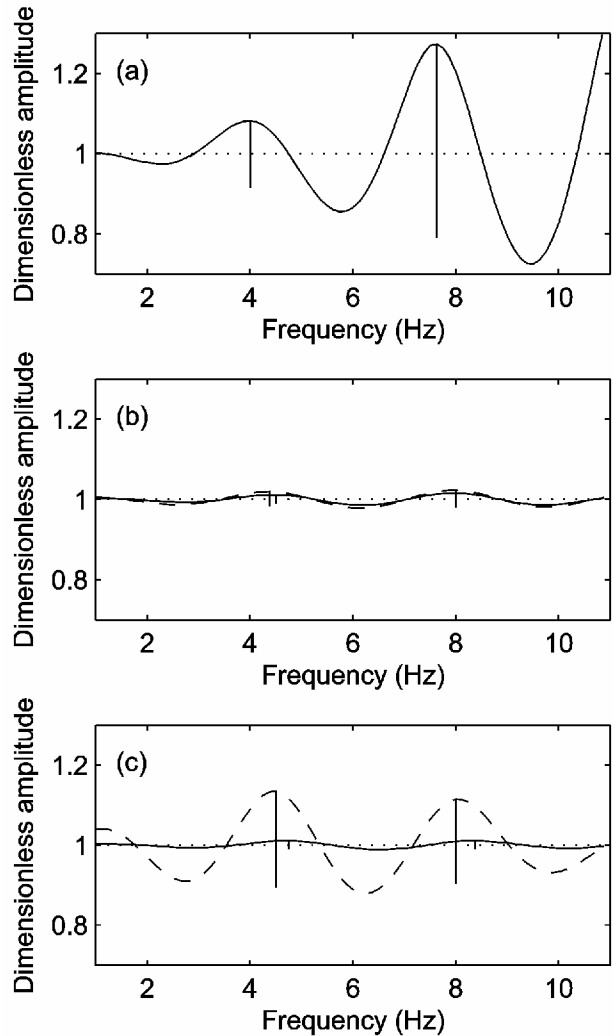


Figure 2. Normalized spectra of solid particle-velocity at the receiver position for 2 (a), 32 (b), and 500 layers (c). In all figures, the dotted lines correspond to the spectra recorded in the absence of layers (homogeneous background medium). The solid and dashed curves correspond to the elastic and poroelastic spectra, respectively. In (a), elastic and poroelastic curves are identical and superposed. The vertical lines represent the measured peak strengths at about 4 Hz and 8 Hz, which are identical for poroelastic and elastic spectra in the case of 2 layers.

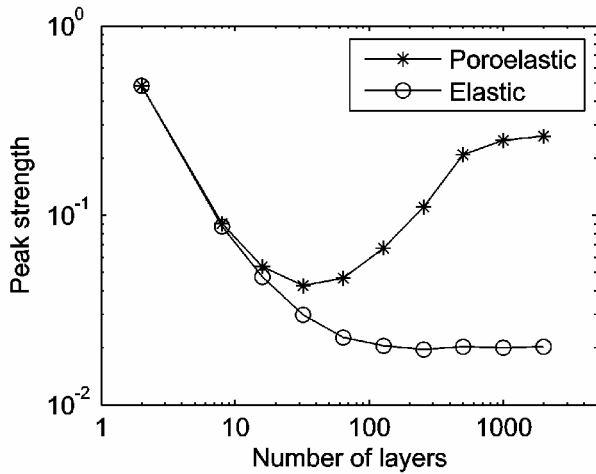


Figure 3. Variation of the peak strength at about 8 Hz (see Figure 3) with increasing number of layers (i.e. decreasing patch size).

Discussion

The amplitude variations of the spectra displayed in Figure 2 are due to constructive and destructive interferences of multiple reflections between the free surface and the reservoir. The results shown in Figures 2 and 3 imply that a reservoir consisting of many thin elastic layers becomes “invisible” in the low-frequency range, which is expected because the effective impedance of the finely layered elastic reservoir, calculated using the Backus average [Backus, 1962; Mavko et al., 1998], is similar to the impedance of the background medium.

When the layers are poroelastic, the spectral anomalies first decrease and then increase with increasing number of layers (Figures 2 and 3). Increasing the number of layers causes a decrease of the patch size which in turn shifts the velocity dispersion curve to higher frequencies (Figure 4a). As the patch size becomes smaller than the diffusion length scale of fluid flow, the behavior of the poroelastic rocks changes from the no-flow state (i.e. patch size much larger than diffusion length; high-frequency limit) to the quasi-static state (i.e. patch size much smaller than diffusion length; low-frequency limit) [Gelinsky and Shapiro, 1997; Müller and Gurevich, 2004]. The effective P-wave velocity of the layered medium calculated from the poroelastic Backus average [Gelinsky and Shapiro, 1997] in the quasi-static limit is 2499 m/s (the impedance is about $5.68 \times 10^6 \text{ kg/m}^2\text{s}$), while in the no-flow limit it is 2689 m/s (the impedance is about $6.11 \times 10^6 \text{ kg/m}^2\text{s}$) and the P-wave velocity of the background medium is 2607 m/s (the impedance is about $6.15 \times 10^6 \text{ kg/m}^2\text{s}$). Therefore, the impedance contrast between the background medium and the reservoir in the no-flow state is about 0.6% while it is about 7% between the background medium and the reservoir in the quasi-static state.

In the transition zone, between no-flow and quasi-static limits, attenuation and velocity dispersion are significant. This is the case, for example, of 500 poroelastic layers

(patch size of 0.2 m). For such medium, the diffusion length of 0.06 m for water-saturated layers and 0.13 m for gas-saturated layers, using the frequency of 5 Hz, at which the quality factor exhibits a minimum and the dispersion is strong (Figure 4). Attenuation and dispersion are necessarily related, according to the Kramers-Krönig relations [Aki and Richards, 1980].

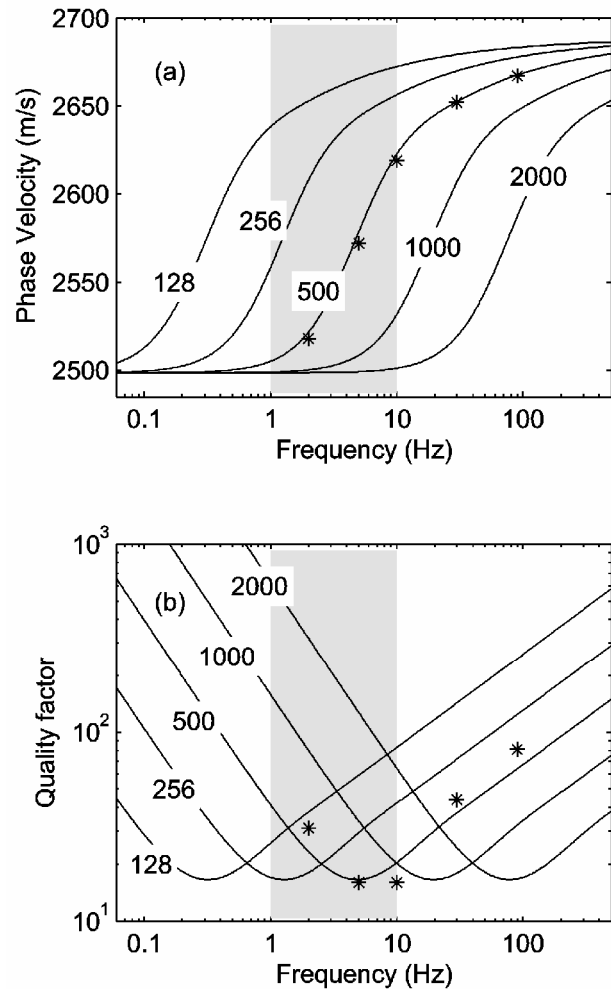


Figure 4. Analytical solution of White's 1D model [Carcione and Picotti, 2006], showing the phase velocity (a) and the quality factor (b) as a function of frequency, for different number of layers (or patch sizes). The star-symbols show values calculated with the finite difference code for a patch size corresponding to 500 layers.

Conclusions

Attenuation due to wave induced flow can cause significant attenuation and velocity dispersion in the low frequency range and within a narrow frequency band (1-10 Hz) for realistic petrophysical parameters (Figure 4). The change of the P-wave velocity from the high- to the low-frequency limit, which is caused by a change in size of the water- and gas-saturated patches, significantly alters the reflectivity of a partially saturated reservoir. The

described effects do not appear in purely elastic models and, therefore, poroelastic models should be applied when studying low-frequency reflections from hydrocarbon reservoirs.

The numerical simulations show that the analytical solutions and the corresponding high- and low-frequency limits, strictly valid for unbounded media, can be applied to reservoirs of finite thickness consisting only of a few hundred patches.

The patchy-saturation model presented here provides a physical basis to the phenomenological attenuation model introduced by *Korneev et al.* [2004], and can explain the spectral anomalies observed at low frequencies in thinly-layered reservoirs.

Acknowledgments

This research has been supported by Spectraseis. B. Quintal and S. M. Schmalholz thank Tobias M. Müller for helpful discussions.

References

- Aki, K., and P. G. Richards** (1980), *Quantitative seismology: Theory and methods*, vol. 1, 557 pp., Freeman, San Francisco (CA).
- Backus, G. E.** (1962), Long-wave elastic anisotropy produced by horizontal layering, *J. Geophys. Res.*, 67, 4427-4440.
- Berryman, J. G.** (1980), Long-wavelength propagation in composite elastic media, I. spherical inclusions, *Journal of Acoustical Society of America*, 68, 1809-1819.
- Biot, M. A.** (1962), Mechanics of deformation and acoustic propagation in porous media, *J. App. Phys.*, 33, 1482-1498.
- Bourbié, T., O. Coussy, and B. Zinszner** (1987), *Acoustics of porous media*, Institut Français du Pétrole Publications, 334 pp., Editions Technip, Paris.
- Cadoret, T., G. Mavko, and B. Zinszner** (1998), Fluid distribution effect on sonic attenuation in partially saturated limestones, *Geophysics*, 63, 154-160.
- Carcione, J. M.** (2007), *Wave Fields in Real Media. Theory and numerical simulation of wave propagation in anisotropic, anelastic, porous and electromagnetic media*, 2nd ed. Vol. 38, 538pp., Elsevier, Amsterdam.
- Carcione, J. M., H. B. Helle, and N. H. Pham** (2003), White's model for wave propagation in partially saturated rocks: Comparison with poroelastic numerical experiments, *Geophysics*, 68, 1389-1398.
- Carcione, J. M., and G. Quiroga-Goode** (1995), Some aspects of the physics and numerical modeling of Biot compressional waves, *J. Comput. Acous.*, 3, 261-280.
- Carcione, J. M., and S. Picotti** (2006), P-wave seismic attenuation by slow-wave diffusion: Effects of inhomogeneous rock properties, *Geophysics*, 71, O1-O8.
- Chapman, M., E. Liu, and X. Li** (2006), The influence of fluid-sensitive dispersion and attenuation on AVO analysis, *Geophys. J. Int.*, 167, 89-105.
- Dutta, N. C., and H. Odé** (1979a), Attenuation and dispersion of compressional waves in fluid filled porous rocks with partial gas saturation (White model) – Part I: Results, *Geophysics*, 44, 1777-1788.
- Dutta, N. C., and H. Odé** (1979b), Attenuation and dispersion of compressional waves in fluid filled porous rocks with partial gas saturation (White model) – Part II: Results, *Geophysics*, 44, 1789-1805.
- Gassmann, F.** (1951), Über die elastizität porös medien, *Vierteljahrsschrift der Naturforschenden Gesellschaft in Zurich*, 96, 1-23.
- Gelinsky, S., and S. A. Shapiro** (1997), Poroelastic Backus averaging for anisotropic layered fluid- and gas-saturated sediments. *Geophysics*, 62, 1867-1878.
- Goloshubin, G., C. VanSchuyver, V. Korneev, D. Silin, and V. Vingalov** (2006), Reservoir imaging using low frequencies of seismic reflections, *The Leading Edge*, 25, 527-531.
- Graf, R., S. M. Schmalholz, Y. Podladchikov, and E. H. Saenger** (2006), Passive low frequency spectral analysis: Exploring a new field in geophysics, *World Oil*, 228, 47-52.
- Gurevich, B. and S.L. Lopatnikov** (1995), Velocity and attenuation of elastic waves in finely layered porous rocks, *Geophys. J. Int.*, 121, 933-947.
- Korneev, V. A., G. M. Goloshubin, T. M. Daley, and D. B. Silin** (2006), Seismic low-frequency effects in monitoring fluid-saturated reservoirs, *Geophysics*, 69, 522-532.
- Levander, A. R.** (1988), Fourth-order finite-difference P-SV seismograms, *Geophysics*, 53, 1425-1436.
- Mavko, G., T. Mukerji, and J. Dvorkin** (1998), *The rock physics handbook: Tools for seismic analysis in porous media*, 329 pp., Cambridge University Press, Cambridge.
- Mavko, G., and T. Mukerji** (1998), Bounds on low frequency seismic velocities in partially saturated rocks, *Geophysics*, 63, 918-924.
- Müller, T. M. and B. Gurevich** (2004), One-dimensional random patchy saturation model for velocity and attenuation in porous rocks, *Geophysics*, 69, 1166-1172.
- Norris, A. N.** (1993), Low-frequency dispersion and attenuation in partially saturated rocks, *J. Acoust. Soc. Am.*, 94, 359-370.
- Picotti, S., and J. M. Carcione** (2006), Estimating seismic attenuation (Q) in the presence of random noise, *J. Seism. Expl.*, 15, 165-181.
- Pride, S. R., J. G. Berryman, and J. M. Harris** (2004), Seismic attenuation due to wave-induced flow: *J. Geophys. Res.*, 109, B01201, doi:10.1029/2003JB002639.
- Quan, Y., and J. M. Harris** (1997), Seismic attenuation tomography using the frequency shift method, *Geophysics*, 62, 895-905.
- Toksöz, M. N., D. H. Johnston, and A. Timur** (1979), Attenuation of seismic waves in dry and saturated rocks: I. Laboratory measurements, *Geophysics*, 44, 681-690.

Toms, J., T. M. Müller, R. Ciz, and B. Gurevich (2006), Comparative review of theoretical models for elastic wave attenuation and dispersion in partially saturated rocks, *Soil Dynamics and Earthquake Engineering*, 26, 548-565.

White, J. E. (1975), Computed seismic speeds and attenuation in rocks with partial gas saturation, *Geophysics*, 40, 224-232.

White, J. E., N. G. Mikhaylova, and F. M. Lyakhovitskiy (1975), Low-frequency seismic waves in fluid saturated layered rocks, *Izvestija Academy of Sciences USSR, Physics of the Solid Earth*, 11, 654-659.